Journal of Statistical Physics, Vol. 76, Nos. 5/6, 1994

Probabilistic Approach to Homoclinic Chaos

D. Daems[1] and G. Nicolis[1]

Received January 19, 1994

Three-dimensional systems possessing a homoclinic orbit associated to a saddle focus with eigenvalues $\rho \pm i\omega$, $-\lambda$ and giving rise to homoclinic chaos when the Shil'nikov condition $\rho < \lambda$ is satisfied are studied. The 2D Poincaré map and its 1D contractions capturing the essential features of the flow are given. At homoclinicity, these 1D maps are found to be piecewise linear. This property allows one to reduce the Frobenius–Perron equation to a master equation whose solution is analytically known. The probabilistic properties such as the time autocorrelation function of the state variable x are explicitly derived.

KEY WORDS: Homoclinic chaos; discrete maps; Frobenius–Perron equation; generalized coarse-graining; master equation; time autocorrelation function.

1. INTRODUCTION

It is by now widely recognized that owing to the property of sensitivity to initial conditions, a probabilistic formalism constitutes the natural approach to deterministic chaos. The starting point of this formalism is a Liouville-like equation describing the evolution of the probability density, which for discrete maps is known as the Frobenius–Perron equation[1] and takes the form

$$\rho_{n+1}(x) \equiv \mathscr{P}\rho_n(x) = \int_\Gamma dy\, \delta(x - f(y, \mu))\, \rho_n(y) \tag{1}$$

Here $\rho_n(x)$ is the probability density at time n, Γ the phase space region available to the system, and $f(x, \mu)$ the deterministic evolution law

$$x_{n+1} = f(x_n, \mu) \tag{2}$$

[1] Faculté des Sciences and Center for Nonlinear Phenomena and Complex Systems, Université libre de Bruxelles, 1050 Bruxelles, Belgium.

0022-4715/94/0900-1287$07.00/0

μ being the control parameter. A great deal of progress has been accomplished on the study of the ergodic properties associated to (1)–(2), and, in particular, of the invariant density $\rho_s(x)$. In contrast, the knowledge of the time-dependent properties of the densities remains fragmentary and limited, essentially, to abstract methematical models of piecewise linear maps.[2–6]

An important class of dynamical systems giving rise to deterministic chaos are homoclinic systems, possessing for a particular combination of parameter values a structurally unstable trajectory which is biasymptotic to a fixed point. If the latter is of the saddle-focus type and the eigenvalues of the linearized equations around it satisfy a certain inequality known as the Shil'nikov condition, then it can be established[7] that near homoclinicity the system possesses trajectories which are in one-to-one correspondence with a shift automorphism with an infinite number of symbols. For three-variable systems the existence of a homoclinic orbit allows one to construct a 2D map which captures all these properties. More significantly for the purposes of this investigation, in many instances, this map can be further reduced to a 1D map[8,9] in the form of distinct branches whose number tends to infinity as the distance from homoclinicity goes to zero. Near homoclinicity these branches can be assimilated to straight-line segments, an idealization that seems in particular to fit reasonably well experimental data and model studies of the Belousov–Zhabotinski reaction.[9,10] One therefore disposes, in this sense, of examples of realistic continuous-time dynamical systems that underly the particular class of the above-described one-dimensional piecewise linear mappings. Our principal goal in the present paper is to work out a probabilistic description of homoclinic systems in which this piecewise linearization at the level of the Poincaré map is adopted.

In Section 2 we study the Frobenius–Perron operator for piecewise linear maps, limiting ourselves to the space of piecewise linear densities. We show that this generalized coarse-graining procedure[3,4,11] reduces the Frobenius–Perron equation to a master equation governed by a stochastic transition matrix. In Section 3 we compute the principal properties concerning the time-dependent behavior of such densities and in particular we show that the generalized coarse-graining introduced suffices to evaluate exactly the time autocorrelation function of the variable x. In Section 4 we derive the explicit form of 1D maps for the spiral and screw types of attractors associated to homoclinic chaos. In Section 5 we consider examples for each of these types of attractor and derive the corresponding master equation. We compute the time autocorrelation function explicitly and compare the analytic results with those of direct numerical solution of the dynamical system. The main conclusions of the work are drawn in Section 6.

2. REDUCTION OF FROBENIUS–PERRON EQUATION TO A MASTER EQUATION FOR PIECEWISE LINEAR DENSITIES

Consider a 1D endomorphism of the form (2), whose states x belong to the interval I. Let $\{C_i\}$, $i=1,\ldots, M$, be a partition of I into M non-overlapping cells

$$\bigcup_{i=1}^{M} C_i = I$$
$$C_i \cap C_j = \varnothing, \qquad i \neq j \tag{3}$$

such that each cell is mapped by the transformation f on a union of cells. We thus require that

$$\chi_{f(C_j)} = \sum_{i=1}^{N} a_{ji} \chi_{C_i}, \qquad j=1,\ldots, M \tag{4}$$

where $\chi_{C_i}(x)$ is the characteristic function of cell C_i, and the elements a_{ji} of the topological transition matrix are 1 or 0, depending on whether C_i belongs or not to $f(C_j)$. Let us consider a piecewise linear initial density $\rho_0(x)$:

$$\rho_0(x) = \sum_{j=1}^{M} \sum_{k=0}^{1} \frac{\alpha_0^{(k)}(j)}{\mu_j^{(k)}} x^k \chi_{C_j}(x) \tag{5}$$

where

$$\mu_j^{(k)} = \int_{C_j} dx\, x^k \tag{6}$$

and the coefficients $\{\alpha_0^{(k)}(j)\}$ determine the probability $P_0(j)$ to find the system in cell C_j at time 0,

$$P_0(j) \equiv \int_{C_j} dx\, \rho_0(x) = \sum_{k=0}^{1} \alpha_0^{(k)}(j) \tag{7}$$

subject to the normalization condition

$$\sum_{j=1}^{M} P_0(j) = \sum_{j=1}^{M} \sum_{k=0}^{1} \alpha_0^{(k)}(j) = 1 \tag{8}$$

The action of the Frobenius–Perron operator $\mathscr{P}$, Eq. (1), on a coarse-grained $\rho_0(x)$ in the sense of Eq. (5) yields

$$\rho_1(x) = \sum_{j=1}^{M} \sum_{k=0}^{1} \sum_{\alpha} \frac{1}{|f'(f_\alpha^{-1}(x))|} \frac{\alpha_0^{(k)}(j)}{\mu_j^{(k)}} (f_\alpha^{-1}(x))^k \chi_{C_j}(f_\alpha^{-1}(x)) \tag{9}$$

We notice that the contribution to the sum over branches f_α^{-1}, $\alpha = 1, 2,...,$ of the inverse transformation is nonvanishing only if $x \in f(C_j)$. If $C_i \subset f(C_j)$, we shall denote by $f_{\alpha(i\to j)}^{-1}$ those branches which map points of C_i back into C_j. By virtue of Eq. (4), Eq. (9) becomes

$$\rho_1(x) = \sum_{i,j=1}^{M} \sum_{k=0}^{1} \sum_{\alpha(i\to j)} \frac{1}{|f'(f_{\alpha(i\to j)}^{-1}(x))|} \frac{\alpha_0^{(k)}(j)}{\mu_j^{(k)}} (f_{\alpha(i\to j)}^{-1}(x))^k a_{ji} \chi_{C_i}(x)) \tag{10}$$

In general, the probability density defined by this equation is not piecewise linear. However, for piecewise linear maps

$$f(x) = \Lambda_{j_{\alpha(i\to j)}} x + \Delta_{j_{\alpha(i\to j)}}, \qquad x \in C_j \tag{11}$$

where $\Lambda_{j_{\alpha(i\to j)}}$ and $\Delta_{j_{\alpha(i\to j)}}$ are constants, so that

$$f_{\alpha(i\to j)}^{-1}(x) = \frac{x - \Delta_{j_{\alpha(i\to j)}}}{\Lambda_{j_{\alpha(i\to j)}}} \tag{12}$$

$$\frac{1}{|f'(f_{\alpha(i\to j)}^{-1}(x))|} = \frac{1}{|\Lambda_{j_{\alpha(i\to j)}}|} \tag{13}$$

It follows that the density $\rho_1(x)$ is again piecewise linear,

$$\rho_1(x) = \sum_{i=1}^{M} \sum_{k=0}^{1} \frac{\alpha_1^{(k)}(i)}{\mu_i^{(k)}} x^k \chi_{C_i}(x) \tag{14}$$

where

$$\alpha_1^{(0)}(i) = \sum_{j=1}^{M} \sum_{\alpha(i\to j)} \frac{\mu_i^{(0)}}{|\Lambda_{j_{\alpha(i\to j)}}|} a_{ji} \left[\frac{\alpha_0^{(0)}(j)}{\mu_j^{(0)}} - \frac{\Delta_{j_{\alpha(i\to j)}} \alpha_0^{(1)}(j)}{\Lambda_{j_{\alpha(i\to j)}} \mu_j^{(1)}} \right] \tag{15}$$

$$\alpha_1^{(1)}(i) = \sum_{j=1}^{M} \sum_{\alpha(i\to j)} \frac{\mu_i^{(1)}}{\mu_j^{(1)}} a_{ji} \frac{1}{|\Lambda_{j_{\alpha(i\to j)}}| \, \Lambda_{j_{\alpha(i\to j)}}} \alpha_0^{(1)}(j) \tag{16}$$

These last relations can be conveniently written as

$$\alpha_1 = \mathbf{W} \cdot \alpha_0 \tag{17}$$

Here α_n, $n = 0, 1,...,$ is a $2M$-component column vector

$$\alpha_n = \begin{pmatrix} \alpha_n^{(0)}(1) \\ \vdots \\ \alpha_n^{(0)}(M) \\ \alpha_n^{(1)}(1) \\ \vdots \\ \alpha_n^{(1)}(M) \end{pmatrix} \tag{18}$$

and $\mathbf{W}$ is a $2M \times 2M$ block upper triangular matrix

$$\mathbf{W} = \begin{pmatrix} \mathbf{W}^{(0)} & \mathbf{W}^{(\times)} \\ 0 & \mathbf{W}^{(1)} \end{pmatrix} \tag{19}$$

with components

$$\begin{aligned} w_{ij}^{(0)} &= \frac{\mu_i^{(0)}}{\mu_j^{(0)}} a_{ji} \sum_{\alpha(i \to j)} \frac{1}{|\Lambda_{j_{\alpha(i \to j)}}|} \\ w_{ij}^{(1)} &= \frac{\mu_i^{(1)}}{\mu_j^{(1)}} a_{ji} \sum_{\alpha(i \to j)} \frac{1}{|\Lambda_{j_{\alpha(i \to j)}}| \, \Lambda_{j_{\alpha(i \to j)}}} \\ w_{ij}^{(\times)} &= \frac{-\mu_i^{(0)}}{\mu_j^{(1)}} a_{ji} \sum_{\alpha(i \to j)} \frac{\Delta_{j_{\alpha(i \to j)}}}{|\Lambda_{j_{\alpha(i \to j)}}| \, \Lambda_{j_{\alpha(i \to j)}}} \end{aligned} \tag{20}$$

After n iterations, the state of the system is entirely described by the density vector α_n, obtainable from the equation

$$\alpha_n = \mathbf{W}^n \cdot \alpha_0 \tag{21}$$

We shall refer to this relation as the generalized master equation. As the Frobenius–Perron operator conserves the norm and the positivity of probability densities, the transition probability matrix $\mathbf{W}$ is stochastic. By Perron's theorem there is then exactly one eigenvalue unity.

The triangular structure of $\mathbf{W}$ implies that if $\lambda_i^{(k)}$ is eigenvalue of $\mathbf{W}^{(k)}$ with $|\lambda_i^{(k)}| \geqslant |\lambda_{i'}^{(k)}|$ for $i < i'$, it is also eigenvalue of $\mathbf{W}$. Let us denote by $\mathbf{u}_{i+kM}$ the eigenvector of $\mathbf{W}$ corresponding to the eigenvalue $\lambda_i^{(k)}$. If all eigenvectors of $\mathbf{W}$ are linearly independent, that is,

$$\sum_{l=1}^{2M} a_l \mathbf{u}_l = 0 \Rightarrow a_l = 0 \quad \forall l \tag{22}$$

they form a basis in which the initial vector α_0 can be decomposed:

$$\alpha_0 = \sum_{i=1}^{M} \sum_{k=0}^{1} a_i^{(k)} \mathbf{u}_{i+kM} \tag{23}$$

By the generalized master equation (21), the density vector at time n is then given by

$$\alpha_n = \sum_{i=1}^{M} \sum_{k=0}^{1} \lambda_i^{(k)n} a_i^{(k)} \mathbf{u}_{i+kM} \tag{24}$$

where the coefficients $\{a_i^{(k)}\}$ are determined by inversion of Eq. (23).

3. ANALYTIC CONSTRUCTION OF THE TIME AUTOCORRELATION FUNCTION

Having at our disposal the formal expression of the probability density at any time [Eq. (21) or (24)], we are in the position to evaluate the statistical properties of the system and, in particular, to compute the time autocorrelation function of various observables of interest.

Let $\Theta(x)$ denote the general form of an observable. By definition, its time autocorrelation function is

$$C(n)=\frac{1}{\sigma^2}\lim_{N\to\infty}\frac{1}{N}\sum_{m=0}^{N-1}[\Theta(x_m)-\bar{\Theta}][\Theta(x_{m+n}-\bar{\Theta}] \tag{25}$$

where $\bar{\Theta}$ and σ^2 are, respectively, the mean value and the variance of Θ. For ergodic transformations this expression can also be written as

$$C(n)=\frac{1}{\sigma^2}\int_I dx\,\rho_s(x)[\Theta(x)-\bar{\Theta}][\Theta(f^n(x))-\bar{\Theta}] \tag{26}$$

where $\rho_s(x)$ is the invariant density, or, introducing the Frobenius–Perron operator,

$$C(n)=\frac{1}{\sigma^2}\int_I dx\,[\Theta(x)-\bar{\Theta}]\,\mathscr{P}^n[\Theta(x)-\bar{\Theta}]\,\rho_s(x) \tag{27}$$

To evaluate this expression we limit ourselves to observables $\Theta(x)$ that are piecewise linear functions of x, which includes as a particular case the time autocorrelation function of the variable x. Proceeding as in the previous section, we therefore write the function $[\Theta(x)-\bar{\Theta}]\,\rho_s(x)$, which we regard as an initial nonequilibrium density, as

$$[\Theta(x)-\bar{\Theta}]\,\rho_s(x)=\sum_{j=1}^{M}\sum_{k=0}^{1}\frac{\alpha_0^{(k)}(j)}{\mu_j^{(k)}}x^k\chi_{C_j}(x) \tag{28}$$

and deduce from the generalized master equation [Eq. (21) or (24)] the nth iterate of the Frobenius–Perron operator on that function,

$$\mathscr{P}^n[\Theta(x)-\bar{\Theta}]\,\rho_s(x)=\sum_{j=1}^{M}\sum_{k=0}^{1}\frac{\alpha_n^{(k)}(j)}{\mu_j^{(k)}}x^k\chi_{C_j}(x) \tag{29}$$

Substituting Eq. (29) into Eq. (27) and performing the integration over x, one then arrives at a formal expression of the time autocorrelation function of the observable $\Theta(x)$ for any given $\Theta(x)$ and piecewise linear map having

the properties summarized by Eqs. (4) and (11). Hereafter, we consider explicitly two cases of special interest where the observable $\Theta(x)$ is:

- The state variable x itself, $\Theta(x) = x$.
- A symbol s taking a constant value within each element of the partition, $\Theta(x) = \sum_{j=1}^{M} s(j)\, \chi_{C_j}(x)$.

3.1. The Observable $\Theta(x) = x$

In this case, the product $[\Theta(x) - \bar{\Theta}]\, \rho_s(x)$ is equal to

$$(x - \bar{x})\, \rho_s(x) = \sum_{j=1}^{M} \frac{u_{j1}}{\mu_j^{(0)}} (x - \bar{x})\, \chi_{C_j} \tag{30}$$

Comparison with Eq. (28) yields

$$\begin{cases} \alpha_0^{(0)}(j) = -\bar{x} u_{j1} \\ \alpha_0^{(1)}(j) = \dfrac{\mu_j^{(1)}}{\mu_j^{(0)}} u_{j1} \end{cases} \qquad j = 1, \ldots, M \tag{31}$$

From these relations, the coefficients $\{a_i^{(k)}\}$ of Eq. (23) and consequently the density vector α_n [Eq. (24)] can be computed. The time autocorrelation function [Eq. (27)] takes then the explicit form

$$C(n) = \sum_{j=1}^{M} \sum_{k=0}^{1} c_j^{(k)} \lambda_j^{(k)n} \tag{32}$$

where

$$c_j^{(k)} = \frac{1}{\sigma^2} \sum_{i=1}^{M} \sum_{l=0}^{1} a_j^{(k)} u_{i+lM, j+kM} \frac{\mu_i^{(l+1)}}{\mu_i^{(l)}} [1 - \delta_{j1} \cdot \delta_{k0}] \tag{33}$$

3.2. The Observable $\Theta(x) = \sum_{j=1}^{M} s(j)\, \chi_{C_j}(x)$

In this case, the product $[\Theta(x) - \bar{\Theta}]\, \rho_s(x)$ is equal to

$$\left[\sum_{j=1}^{M} s(j)\, \chi_{C_j} - \bar{s} \right] \rho_s(x) = \sum_{j=1}^{M} [s(j) - \bar{s}] \frac{u_{j1}}{\mu_j^{(0)}} \chi_{C_j} \tag{34}$$

Comparison with Eq. (28) yields

$$\begin{cases} \alpha_0^{(0)}(j) = u_{j1}[s(j) - \bar{s}] \\ \alpha_0^{(1)}(j) = 0 \end{cases} \qquad j = 1, \ldots, M \tag{35}$$

From these relations, the coefficients $\{a_i^{(k)}\}$ of Eq. (23) can be computed. Note that the transition probability matrix $\mathbf{W}$ being block upper triangular, its eigenvectors corresponding to eigenvalues $\{\lambda_i^{(0)}\}$ have their M last components vanishing:

$$u_{j+M,i} = 0, \qquad i, j = 1, \ldots, M \tag{36}$$

Consequently, the second half of Eq. (35) implies, by virtue of the linear independence of the eigenvectors of $\mathbf{W}$ [Eq. (22)], that the coefficients $\{a_i^{(1)}\}$ vanish. The density vector α_n [Eq. (24)] depends therefore only on the eigenvalues $\{\lambda_i^{(0)}\}$. It follows that the time autocorrelation function of the piecewise constant observable s [Eq. (27)] takes the explicit form

$$C(n) = \sum_{j=1}^{M} c_j^{(0)} \lambda_j^{(0)n} \tag{37}$$

where

$$c_j^{(0)} = \frac{1}{\sigma^2} \sum_{i=1}^{M} a_j^{(0)} u_{ij} s(j)[1 - \delta_{j1}] \tag{38}$$

4. HOMOCLINIC CHAOS: THE SHIL'NIKOV MAP AND ITS 1D CONTRACTION

Consider the three-variable continuous time dynamical system

$$\begin{cases} \dot{x} = \rho_\mu x + \omega_\mu y + P_\mu(x, y, z) \\ \dot{y} = \omega_\mu x + \rho_\mu y + Q_\mu(x, y, z) \\ \dot{z} = -\lambda_\mu z + R_\mu(x, y, z) \end{cases} \tag{39}$$

where μ is a control parameter and P_μ, Q_μ, R_μ are analytic functions in x, y, z, and μ, vanishing together with their first derivatives in $(0, 0, 0)$. We suppose that the origin behaves as a saddle-focus ($\lambda_\mu > 0$, $\rho_\mu > 0$), that there exists for $\mu = 0$ a homoclinic orbit Γ_0 biasymptotic to the origin, and that the inequality $\rho_0 < \lambda_0$ is satisfied. Under these conditions the Shil'nikov theorem[7] asserts that the flow contains a subset of chaotic trajectories in the sense specified in the introduction.

Although a homoclinic orbit is structurally unstable, for parameter values near those characterizing the homoclinic situation a general pattern of reinjection of trajectories near the saddle-focus should subsist. This property allows one to construct a two-dimensional mapping capturing the essential features of the flow. To this end, we assume that it is possible to

carry out a C^3 coordinate transformation which linearizes (39) near the origin. In a neighborhood V of this point, the equations in new coordinates (denoted for simplicity as the old ones) take the form

$$\begin{cases} \dot{x} = \rho_\mu x - \omega_\mu y \\ \dot{y} = \omega_\mu x - \rho_\mu y \\ \dot{z} = -\lambda_\mu z \end{cases} \tag{40}$$

The local unstable manifold of the saddle focus is now the x–y plane, whereas the stable one is the z axis. The Poincaré map in a plane transverse to the local stable manifold is then obtained as the composition of two transformations. The first one, which accounts for the behavior near the saddle-focus, is obtained by straightforward integration of the linear equations (40), whereas the second one, which is responsible for the reinjection of the dynamics in the vicinity of the fixed point, is assumed to be an isometric transport. One arrives thus at the two-dimensional mapping[9,10]

$$\begin{cases} x' = [(x^2+y^2)^{1/2}\,\xi_\mu^\kappa - x^*]\cos\varphi - h\xi_\mu^{-(\lambda_\mu/\rho_\mu)\kappa}\sin\varphi + \hat{x}_\mu \\ y' = [(x^2+y^2)^{1/2}\,\xi_\mu^\kappa - x^*]\sin\varphi + h\xi_\mu^{-(\lambda_\mu/\rho_\mu)\kappa}\cos\varphi + \hat{y}_\mu \end{cases} \qquad x, y \in \mathscr{D} \tag{41}$$

where

$$\xi_\mu = e^{-\pi\rho_\mu/\omega_\mu}, \qquad \kappa = \frac{[1-\mathrm{sgn}(x)]}{2} - 2k + \frac{1}{\pi}\arctan\frac{y}{x}$$

and $\mathscr{D}$ is the inner domain delimited by the arc of spiral $r = \tilde{x}\xi_\mu^{2-\theta/\pi}$, $0 \leqslant \theta < 2\pi$, and the segment joigning its extremities. In this expression, x^* and h define the points $(x^*, 0, 0)$ and $(0, 0, h)$ where the homoclinic orbit respectively leaves and enters the neighborhood V; $\tilde{x}$ is such that $\tilde{x}\xi_\mu^2 \leqslant x^* \leqslant \tilde{x}$; $\hat{x}_\mu$ and $\hat{y}_\mu$ describe the distance from homoclinicity ($\hat{x}_0 = 0$, $\hat{y}_0 = 0$); φ accounts for a rotation during the rigid transport; and k is an integer which corresponds to the number of turns the trajectory completes around the saddle-focus between two successive intersections of the Poincaré plane. In the infinite area contraction limit ($h/x^* \to 0$) and choosing for simplicity $\varphi = 0$, (41) reduces to the one-dimensional map

$$x' = (x^2+\hat{y}^2)^{1/2}\,\xi^\kappa + \hat{x} - 1, \qquad \tilde{x}\xi^2 + \hat{x} - 1 < x \leqslant \tilde{x} + \hat{x} - 1 \tag{42}$$

Here x, $\tilde{x}$, $\hat{x}$, and $\hat{y}$ denote, respectively, a new variable and new control parameters, equal to the old ones divided by x^*. A detailed analysis of this globally highly nonlinear law reveals two qualitatively different types of maps:

(i) A map in the form of nonoverlapping increasing or decreasing linear branches whose number tends to infinity as the distance from homoclinicity, or more precisely, the new parameter $\hat{x}$ tends to zero

$$f_s(x) = x\,\mathrm{sgn}(x)\,\xi^{[1-\mathrm{sgn}(x)]/2-2k} + \hat{x} - 1$$
$$\hat{x} + (\xi^2 - 1)\frac{1-\mathrm{sgn}(x)}{2} \leqslant x < \hat{x} + \left(\frac{1}{\xi^2} - 1\right)\frac{1+\mathrm{sgn}(x)}{2} \tag{43}$$

Since each branch corresponds to a given even or odd number number of half-turns of the trajectory around the origin between two crossings of the Poincaré surface, this type of map describes a spiral-type attractor.[2]

(ii) A map which at homoclinicity exhibits two infinite sequences of decreasing and increasing branches. At finite distance from homoclinicity, these two families of branches are finite and separated by a quadratric well which becomes deeper as the system evolves to homoclinicity.

$$f_t(x) = x\,\mathrm{sgn}(x)\,\xi^{[1-\mathrm{sgn}(x)]/2-2k+(1/\pi)\arctan(\hat{y}/x)}\left(1+\frac{\hat{y}^2}{x^2}\right)^{1/2} - 1$$
$$\tilde{x}\xi^2 - 1 < x \leqslant \tilde{x} - 1 \tag{44}$$

As this map allows for reinjection on both sides of the origin, it describes a screw-type attractor.

Notice that at homoclinicity both maps turn out to be piecewise linear. In the sequel the statistical properties of the two types of attractors generated by the dynamical system (42) will be explored by adopting the simplification that the piecewise linear character of the maps extends in a certain vicinity of homoclinicity as well.

5. PROBABILISTIC DESCRIPTION OF THE PIECEWISE LINEAR 1D CONTRACTION OF THE SHIL'NIKOV MAP

As shown in Section 2, in addition to the requirement of piecewise linear maps, the reduction of the Frobenius–Perron equation to a master equation relies on the property that the phase space partition be such that

[2] At homoclinicity, the reinjections of the dynamics in the x–y plane are made along a line passing by the origin. By definition, for the spiral-type attractor the reinjections occur on one side of the origin, whereas for the screw type they occur on both sides.

each of its elements is transformed by the deterministic dynamics into a union of its elements. In this section we build models of spiral- and screw-type attractors compatible with these properties and derive subsequently the master equation and the behavior of the time autocorrelation function of the two classes of observables introduced in Section 3. Hereafter, we consider separately the cases of spiral- and screw-type attractors.

5.1. Spiral-Type Attractor

Let us consider the map (43) when limited to three branches corresponding to 1, 3, and 5 half-turns of the trajectory around the origin ($k = 1, 2, 3$). The 1D map f_s reads then

$$f_s(x) = -\frac{x}{\xi^{2i-1}} + \hat{x} - 1, \qquad b_{i-1} < x \leqslant b_i, \qquad i = 1, 2, 3 \tag{45}$$

We choose

$$\begin{aligned} f_s(C_1) &= C_1 \cup C_2 \\ f_s(C_2) &= C_1 \cup C_2 \cup C_3 \\ f_s(C_3) &= C_2 \cup C_3 \end{aligned} \tag{46}$$

where the partition considered is the one defined by the points of discontinuity, $C_i =]b_{i-1}, b_i]$. One can easily check that these relations imply

$$\begin{aligned} \xi &\simeq 0.67546 \\ \hat{x} &= 1 - \xi^2(1+\xi)(1+\xi^2) \\ b_0 &= \xi^2 + \hat{x} - 1 \\ b_1 &= -\xi^3 \\ b_2 &= -\xi^5 \\ b_3 &= \hat{x} \end{aligned} \tag{47}$$

As this map satisfies conditions (4) and (11), the action of the Frobenius–Perron operator can be reduced to the iteration of a stochastic matrix. Taking into account Eqs. (45)–(47), this transition probability matrix, whose elements are given by Eqs. (20), reads

$$\mathbf{W} = \begin{pmatrix}
\xi & \frac{\xi^4}{1-\xi} & 0 & \frac{2(1+\xi)(1-\hat{x})}{\xi(2+3\xi+2\xi^2+\xi^3)} & \frac{2\xi^4(1-\hat{x})}{(1-\xi)(1+\xi^2)} & 0 \\
1-\xi & \xi^3 & \frac{\xi^8(1-\xi)}{1-\xi-\xi^3} & \frac{2(1-\xi^2)(1-\hat{x})}{\xi^2(2+3\xi+2\xi^2+\xi^3)} & \frac{2\xi^3(1-\hat{x})}{1+\xi^2} & \frac{2\xi^{13}(1-\xi^2)(\hat{x}-1)}{\hat{x}^2-\xi^{10}} \\
0 & \frac{1-\xi-\xi^3}{1-\xi} & \xi^5 & 0 & \frac{2(1-\hat{x})(\hat{x}+\xi^5)}{1-\xi^4} & \frac{2\xi^{10}(\hat{x}-1)}{\hat{x}-\xi^5} \\
0 & 0 & 0 & -\xi^2 & \frac{\xi^7(2+3\xi+2\xi^2+\xi^3)}{\xi^4-1} & 0 \\
0 & 0 & 0 & \frac{\xi(\xi^4-1)}{2+3\xi+2\xi^2+\xi^3} & -\xi^6 & \frac{\xi^{16}(\xi^4-1)}{\xi^{10}-\hat{x}^2} \\
0 & 0 & 0 & 0 & \frac{\hat{x}^2-\xi^{10}}{1-\xi^4} & -\xi^{10}
\end{pmatrix} \tag{48}$$

Densities evolve then according to the master equation (21) or (24). The eigenvalues of $\mathbf{W}$ are all real,

$$\begin{aligned}
\lambda_1^{(0)} &= 1 & \lambda_1^{(1)} &= -0.552 \\
\lambda_2^{(0)} &= 0.244 & \lambda_2^{(1)} &= -0.050 \\
\lambda_3^{(0)} &= -0.120 & \lambda_3^{(1)} &= 0.031
\end{aligned} \tag{49}$$

The invariant eigenvector reads

$$\mathbf{u}_1 = \begin{pmatrix} 0.651 \\ 0.330 \\ 0.019 \\ 0 \\ 0 \\ 0 \end{pmatrix} \tag{50}$$

From Eq. (24), we deduce that α_s is equal to $\mathbf{u}_1$, so that the stationary density is

$$\rho_s(x) = 1.87\chi_{C_1}(x) + 1.97\chi_{C_2}(x) + 0.70\chi_{C_3}(x) \tag{51}$$

This expression allows one to compute the average value of various quantities and to check that the 1D map (45) displays sensitivity to initial

conditions with a Lyapunov exponent equal to 0.681. Let us focus on the time autocorrelation function of the observables considered in Section 3.

5.1.1. The Observable $\Theta(x)=x$. From Eq. (32) applied to the transition probability matrix **W** of Eq. (48) we deduce that the time autocorrelation function of the x-observable decays as

$$C(n)=\sum_{j=1}^{3}\sum_{k=0}^{1} c_j^{(k)}\lambda_j^{(k)n} \tag{52}$$

where

$$\begin{aligned} c_1^{(0)}&=0 & c_1^{(1)}&=0.927\\ c_2^{(0)}&=0.180 & c_2^{(1)}&=0.024\\ c_3^{(0)}&=-0.128 & c_3^{(1)}&=-0.003 \end{aligned} \tag{53}$$

In Fig. 1, a comparison is made between the analytical expression (52) and the numerical data obtained by computing the time autocorrelation function from the trajectory according to Eq. (25).

5.1.2. The Observable $\Theta(x)=\sum_{j=1}^{M} s(j)\,\chi_{C_j}(x)$. A discrete observable of interest in the context of homoclinic systems is the number of half-turns the trajectory completes in the vicinity of the saddle-focus between two successive intersections of the Poincaré plane. For the map f_s, this observable is expressed as

$$\Theta(x)=1\chi_{C_1}(x)+3\chi_{C_2}(x)+5\chi_{C_3}(x) \tag{54}$$

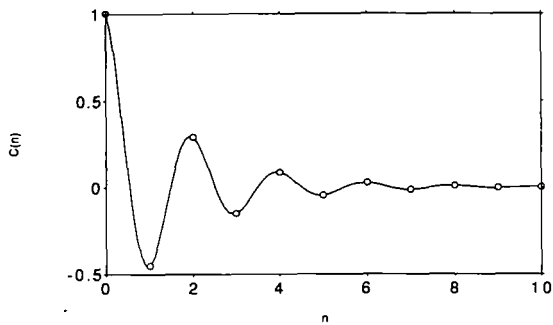

Fig. 1. Comparison between the analytical expression of the time autocorrelation function of the observable x (solid line) and the numerical data obtained by computing this function from the trajectory (dots) for a spiral type of attractor. The numerical autocorrelation function shown was obtained by averaging 5000 autocorrelation functions of length $N=1000$.

Its time autocorrelation function, which is given by Eq. (37), is found to decay as

$$C(n) = \sum_{j=1}^{3} c_j^{(0)} \lambda_j^{(0)n} \tag{55}$$

where

$$\begin{aligned} c_1^{(0)} &= 0 \\ c_2^{(0)} &= 0.232 \\ c_3^{(0)} &= 0.768 \end{aligned} \tag{56}$$

In Fig. 2, a comparison is made between the analytical expression (55) and the numerical data obtained from Eq. (25).

5.2. Screw-Type Attractor

Let us restrict the 1D map f_v [Eq. (44)] to two branches $k = 1$ and one well $k = 2$. We also choose

$$\begin{aligned} \bar{f}_v(C_1) &= C_1 \cup C_2 \cup C_3 \cup C_4 \\ \bar{f}_v(C_2) &= C_4 \\ \bar{f}_v(C_3) &= C_4 \\ \bar{f}_v(C_4) &= C_1 \cup C_2 \cup C_3 \cup C_4 \end{aligned} \tag{57}$$

where $\bar{f}_v$ denotes the piecewise linear map obtained by neglecting the terms in $\hat{y}/x$ in the two branches of f_v and by replacing the well by two segments of straight line passing by its minimum. As above, the partition is deter-

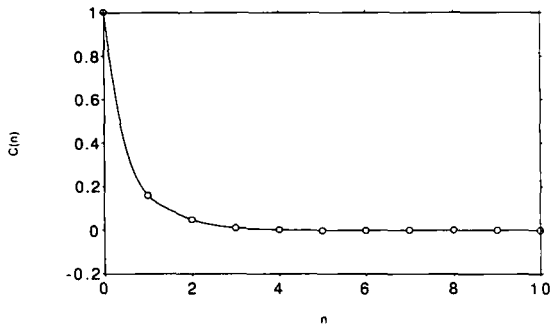

Fig. 2. Comparison between the analytical expression of the time autocorrelation function of the piecewise constant observable s (solid line) and the numerical data obtained by computing this function from the trajectory (dots) for a spiral type of attractor. The numerical autocorrelation function was obtained as in Fig. 1.

mined by the points of discontinuity, $C_i =]b_{i-1}, b_i]$. The map $\bar{f}_v(x)$ reads then

$$\bar{f}_v(x) = \begin{cases} -2x - 1 & b_0 < x \leqslant b_1 \\ \dfrac{1}{\beta - 1} x + \dfrac{2\beta - 1}{6(\beta - 1)} & b_1 < x \leqslant b_2 \\ \dfrac{1}{\beta} x + \dfrac{4\beta - 1}{12\beta} & b_2 < x \leqslant b_3 \\ 4x - 1 & b_3 < x \leqslant b_4 \end{cases} \tag{58}$$

where

$$\begin{aligned} b_0 &= -\frac{2}{3} & b_3 &= \frac{1}{12} \\ b_1 &= -\frac{1}{6} & b_4 &= \frac{1}{3} \\ b_2 &= \frac{13 \ln 2}{192\pi\{1 + [\ln 2/\pi]^2\}^{1/2} 2^{(1/\pi)\arctan(\pi/\ln 2)}} & \beta &= \frac{b_2 - b_3}{b_3 - b_4} \end{aligned} \tag{59}$$

By construction this map satisfies conditions (4) and (11), so that densities evolve according to the master equation (21) or (24). Taking into account Eqs. (57)–(59), we have for the transition probability matrix **W**, whose elements are given by Eqs. (20),

$$\mathbf{W} = \begin{pmatrix} \frac{1}{2} & 0 & 0 & \frac{1}{2} & \frac{3}{5} & 0 & 0 & \frac{3}{5} \\ \frac{1-\beta}{4} & 0 & 0 & \frac{1-\beta}{4} & \frac{3(1-\beta)}{10} & 0 & 0 & \frac{3(1-\beta)}{10} \\ \frac{\beta}{4} & 0 & 0 & \frac{\beta}{4} & \frac{3\beta}{10} & 0 & 0 & \frac{3\beta}{10} \\ \frac{1}{4} & 1 & 1 & \frac{1}{4} & \frac{3}{10} & \frac{4(2\beta^2 - 3\beta + 1)}{3\beta^2 - 2\beta - 1} & \frac{2 - 8\beta}{2 - 3\beta} & \frac{3}{10} \\ 0 & 0 & 0 & 0 & -\frac{1}{4} & 0 & 0 & -\frac{1}{4} \\ 0 & 0 & 0 & 0 & \frac{3\beta^2 - 2\beta - 1}{80} & 0 & 0 & \frac{3\beta^2 - 2\beta - 1}{80} \\ 0 & 0 & 0 & 0 & \frac{\beta(2 - 3\beta)}{80} & 0 & 0 & \frac{\beta(2 - 3\beta)}{80} \\ 0 & 0 & 0 & 0 & \frac{1}{16} & \frac{5(1-\beta)^2}{1 + 2\beta - 3\beta^2} & \frac{5\beta}{2 - 3\beta} & \frac{1}{16} \end{pmatrix} \tag{60}$$

Its spectrum comprises now one pair of complex eigenvalues,

$$\begin{aligned} \lambda_1^{(0)} &= 1 & \lambda_1^{(1)} &= -0.09375 + 0.1321\,i \\ \lambda_2^{(0)} &= -\tfrac{1}{4} & \lambda_2^{(1)} &= -0.09375 - 0.1321\,i \\ \lambda_3^{(0)} &= 0 & \lambda_3^{(1)} &= 0 \\ \lambda_4^{(0)} &= 0 & \lambda_4^{(1)} &= 0 \end{aligned} \tag{61}$$

The invariant eigenvector reads

$$\mathbf{u}_1 = \begin{pmatrix} 0.4 \\ 0.142 \\ 0.058 \\ 0.4 \\ 0 \\ 0 \\ 0 \\ 0 \end{pmatrix} \tag{62}$$

so that the stationary density is

$$\rho_s(x) = \tfrac{4}{5}[\chi_{C_1}(x) + \chi_{C_2}(x) + \chi_{C_3}(x) + 2\chi_{C_4}(x)] \tag{63}$$

From this expression, one can easily check that the 1D map (58) displays sensitivity to initial conditions with a Lyapunov exponent equal to 0.952. Let us turn to the time autocorrelation function of the observables considered above.

5.2.1. The Observable $\Theta(x) = x$. From Eq. (32) applied to the transition probability matrix $\mathbf{W}$ of Eq. (60) we deduce that the autocorrelation function of the x-observable decays as

$$C(n) = \sum_{j=1}^{4} \sum_{k=0}^{1} c_j^{(k)} \lambda_j^{(k)n} \tag{64}$$

where

$$\begin{aligned} c_1^{(0)} &= 0 & c_1^{(1)} &= 0.608 - 0.016\,i \\ c_2^{(0)} &= -0.216 & c_2^{(1)} &= 0.608 + 0.016\,i \\ c_3^{(0)} &= 0 & c_3^{(1)} &= 0 \\ c_4^{(0)} &= 0 & c_4^{(1)} &= 0 \end{aligned} \tag{65}$$

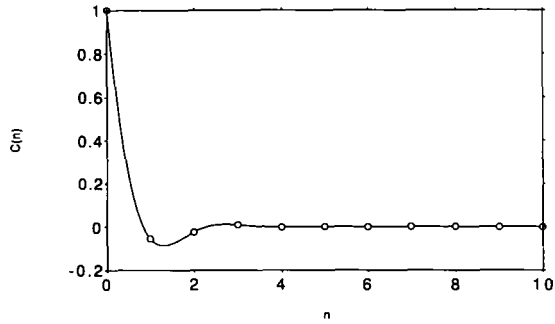

Fig. 3. As in Fig. 1, but for a screw type of attractor.

In Fig. 3, a comparison is made between the analytical expression (64) and the numerical data obtained from the trajectory according to Eq. (25).

5.2.2. The Observable $\Theta(x) = \sum_{j=1}^{M} s(j)\,\chi_{C_j}(x)$. Let us consider as discrete observable the number of half-turns the trajectory completes around the origin between two intersections of the Poincaré plane, or explicitly in the case of map (58),

$$\Theta(x) = 4\chi_{C_1}(x) + 2\chi_{C_2}(x) + 2\chi_{C_3}(x) + 4\chi_{C_4}(x) \tag{66}$$

For such an observable, the time autocorrelation function is given by Eq. (37) and found to depend on lag n as

$$C(n) = \sum_{j=1}^{4} c_j^{(0)} \lambda_j^{(0)n} \tag{67}$$

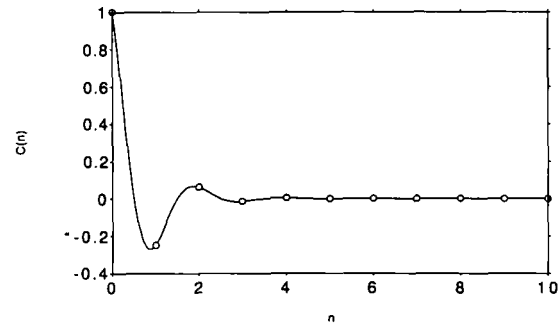

Fig. 4. As in Fig. 2, but for a screw type of attractor.

where

$$\begin{aligned} c_1^{(0)} &= 0 \\ c_1^{(0)} &= 1 \\ c_3^{(0)} &= 0 \\ c_4^{(0)} &= 0 \end{aligned} \tag{68}$$

In Fig 4, a comparison is made between the analytical expression (67) and the numerical data obtained from Eq. (25).

6. CONCLUSIONS

In this paper a probabilistic description of homoclinic systems has been carried out analytically. In particular, the time autocorrelation functions of observables such as the state variable x have been derived for models of the spiral- and screw-type attractors associated to homoclinic chaos. Our results can readily be generalized to piecewise analytic observables and to observables having discontinuities at the elements of periodic orbits.[4] It is also obvious that the formalism used here is not limited to homoclinic systems, but extends to any piecewise linear map having the properties summarized by Eqs. (4) and (11).

In addition to giving quantitative information on the way the dynamics loses its memory, we believe that the decay modes of the time autocorrelation function of the x-observable provide a useful characterization of spiral-type versus screw-type attractor. For the spiral-type attractor, the leading decay rate of the time autocorrelation of the position observable is determined by a negative eigenvalue. This means that the point of reinjection of the flow on the Poincaré plane oscillates around the mean value $\bar{x}$ with period two. For the screw-type attractor, there is also a negative leading eigenvalue, so that the point of reinjection of the flow still oscillates around the mean value $\bar{x}$ with period two. But in addition there exist complex eigenvalues. The point of reinjection oscillates then, on the average, from one side to the other with a more complicated period obtained from the trigonometric representation of the complex eigenvalues. Furthermore, for the examples considered here, the decay modes of the screw type of attractor interfere in a destructive way, whereas for the spiral type they reinforce the oscillation of the leading one. This trend is confirmed by the study of further examples involving higher number of branches. It turns out that several negative eigenvalues of about the same amplitude may exist for both types of attractors. But in the case of the spiral type their effect seems to reinforce that of the leading eigenvalue, whereas for the screw type these negative eigenvalues, eventually together with complex ones, seem to

concel the effect of the leading one. We believe this is due to the coexistence of increasing and decreasing branches which occurs in the 1D map of the screw but not in that of the spiral type of attractor and so finally to the topology of the attractor itself. Furthermore, for both types of attractors it can be shown that when every branch is mapped onto the interval the correlation function is determined by a single non-trivial eigenvalue: $\sum_i 1/(\Lambda_i |\Lambda_i|)$, the magnitude of which is then smaller in the case of the screw-type attractor.[3] Owing to the destructive interference between the decay modes of this type of attractor and to the lowering of the leading one, the time autocorrelation functions of the screw-type attractors appear less organized. As a consequence the power spectra of screw-type attractors have a more pronounced broad band component than those of the spiral type where characteristic frequencies emerge. This is corroborated by power spectrum computation of continuous-time dynamical systems generating as the parameters vary spiral and screw chaos.[12]

ACKNOWLEDGMENTS

The authors thank P. Gaspard and D. McKernan for stimulating discussions and are indebted to F. Argoul for communicating experimental data on the Belousov–Zhabotinski reaction. This work has been supported in part by the Belgian government under the Pôles d'Attraction Interuniversitaires program. D.D. is Aspirant Chercheur at the Fonds National de la Recherche Scientifique (Belgium).

REFERENCES

1. A. Lasota and M. Mackey, *Probabilistic Properties of Deterministic Systems* (Cambridge University Press, Cambridge, 1985).
2. H. Mori, B. So, and T. Ose, *Prog. Theor. Phys.* **66**:4 (1981).
3. G. Nicolis, J. Piasecki, and D. McKernan, Toward a probabilistic description of deterministic chaos, in *From Phase Transitions to Chaos*, G. Györgi, I., Kondor, L. Savári, and T. Tél, eds. (World Scientific, Singapore, 1992).
4. D. McKernan and G. Nicolis, Generalized Markov coarse graining and spectral decompositions of chaotic piecewise linear maps, preprint ULB (1993).
5. P. Gaspard, *J. Phys. A: Math. Gen.* **25**:L483 (1992).
6. I. Antoniou and S. Tasaki, *Physica A* **190**:303 (1993).
7. L. P. Shil'nikov, *Sov. Math. Dokl.* **6**:163 (1965); *Math. USSR Sbornik* **10**:91 (1970).
8. P. Gaspard, R. Kapral, and G. Nicolis, *J. Stat. Phys.* **35**:697 (1984).
9. A. Arnéodo, F. Argoul, J. Elezgaray, and P. Richetti, *Physica D* **62**:134 (1993).
10. P. Richetti, Ph.D. dissertation, University of Bordeaux (1987).
11. G. Nicolis and C. Nicolis, *Phys. Rev. A* **38**:427 (1988).
12. D. Farmer, J. Crutchfield, J. Froehling, N. Packard, and R. Shaw, *Ann. N. Y. Acad. Sci.* **357**:453 (1980).

[3] This property extends to the leading eigenvalue when every branch is not mapped onto the interval.